INFLUENCE OF LASER ABLATION TREATMENT ON ELECTROCHEMICAL CHARACTERISTICS OF AZ80 MAGNESIUM ALLOY

Daniel Kajánek[1,*], Luboš Halimovič[1], Martina Jacková[1], Leoš Doskočil[2], Ingrid Zuziaková[1], Branislav Hadzima[1]

[1]Research Centre, University of Zilina, Zilina, Slovak Republic
[2]Materials Research Centre, Faculty of Chemistry, Brno University of Technology, Brno, Czech Republic

*E-mail of corresponding author: daniel.kajanek@uniza.sk

Daniel Kajánek 0000-0002-5005-8740,
Leoš Doskočil 0000-0002-9584-9191,
Martina Jacková 0000-0003-1625-6847,
Branislav Hadzima 0000-0002-8201-905X

Resume

In this study was investigated the effect of a novel surface treatment technique, called laser ablation or laser surface cleaning (LSC), on the electrochemical properties of AZ80 magnesium alloys. Its effect on corrosion resistance was compared to conventional techniques represented by grinding and polishing. The corrosion stability of the produced surfaces was determined by potentiodynamic (PD) polarization tests and electrochemical impedance spectroscopy in 0.1M NaCl. The results showed that the LSC process produced a regular, uniform surface morphology. Although the LSC treatment led to the passivation of the AZ80 surface, the overall corrosion resistance was compromised compared to surfaces treated by grinding and polishing.

Article info

Received 27 February 2025
Accepted 14 April 2025
Online 30 April 2025

Keywords:

magnesium alloy
corrosion
laser ablation
laser surface cleaning

Available online: https://doi.org/10.26552/com.C.2025.039

ISSN 1335-4205 (print version)
ISSN 2585-7878 (online version)

1 Introduction

Magnesium is one of the most abundant elements on earth, which led to the idea of using magnesium as an engineering metal [1-2]. However, the mechanical properties of magnesium are not very favourable due to its hexagonal lattice [3]. The main advantage of using magnesium as an engineering material is its low density, which is 1.74 g.cm^{-3}. Other positive properties of magnesium are its ratio of tensile strength to density (specific strength) and its non-toxicity, which allows it to be used as a biodegradable implant [4-6]. Magnesium alloys, due to their low density, can reduce the weight of a vehicle, which in turn lowers fuel consumption. This can be achieved by replacement of commonly used materials such as steels. Using of magnesium alloys can subsequently have a positive impact on greenhouse gas emissions. Currently, components made of magnesium alloys, such as engine blocks, central control panels, door frames, steering wheels, etc., are already in use. However, most of these components can be found only in high-end cars like Porsche or Jaguar due to higher economical demands [4].

Despite its promising properties, magnesium and therefore its alloys have a major disadvantage represented by their high electrochemical reactivity in most practical environments [7-8]. This behaviour is mainly indicated by the low standard electrode potential of magnesium (-2.36 vs. SHE). This is the lowest value of the commonly used metals, with the exception of lithium. Another problem with the corrosion resistance of magnesium is the non-protective surface film formed when exposed to the environment. This quasi-passive film is only protective in highly alkaline environments. To overcome this problem, extensive efforts are being made to improve the corrosion resistance of magnesium alloys. One of the ways to improve the corrosion resistance is to alloy magnesium with corrosion resistant materials. However, alloying magnesium with other metals is often unfavourable due to the occurrence of microgalvanic corrosion leading to dissolution of the Mg matrix [8-9]. The more favourable and effective approach is to apply a proper surface treatment. Grinding, polishing or milling and turning are typical representatives of the category of conventional surface treatment methods [10-12]. On the other hand, there are unconventional surface treatment methods whose influence is still the subject of research by many scientific teams. This

category is represented by various coating processes, such as plasma-electrolytic oxidation, chemical vapour deposition (CVD) and physical vapour depositions (PVD) methods, treatments based on the application of laser beams, etc. [13-18].

Laser surface cleaning (LSC), commonly known as laser ablation, is one of the unconventional and novel laser-based surface modification methods for metallic materials. The main difference between LSC and laser surface melting (LSM) is the careful selection of processing parameters to avoid melting of the surface layer [16-18]. The LSC is a non-contact technique that aims to clean and decontaminate the surface from impurities by carefully setting up the laser beam. During the LSC treatment, the concentrated laser beam is generated by the power supply. When the treated surface is hit by the laser beam, energy absorption begins. The removal of impurities or other layers depends on the ability of the surface layer to absorb the energy transferred by the laser beam. In practice, the higher the ability of the surface to absorb energy, the higher the efficiency of the removal process [19]. This method is used when a clear, oxide-free surface is required. The positive effect on surface properties is reported on metallic materials, such as various types of steel, titanium alloys, aluminium alloys, etc. One of the most important advantages of LSC compared to common chemical cleaning of metals is the high environmental friendliness of the whole process [15-16]. Studies on the effect of the LSC on the corrosion resistance of materials have confirmed that in the case of stainless steels or aluminium alloys, e.g. materials that can be passivated, the LSC method proved to be beneficial in improving the corrosion resistance in aggressive environments [20-21]. On the other hand, the application of this method to materials with low melting points, such as zinc, did not have a positive effect on corrosion stability. The researchers stated that the zinc was melted before the oxides were successfully removed [22]. Few studies can be found on the LSC treatment of magnesium alloys. For example, the study by Zhu et al., 2024 dealt with the application of laser cleaning as a pre-treatment to the micro-arc oxidation (MAO) coatings. Although the authors found a positive effect on the corrosion resistance of AZ31 alloy, only a 20 W laser treatment without coating was tested for a short exposure time of 30 minutes [23]. In contrast to this study, Xiong et al., 2024 found that the application of 6.5 W laser treatment had a negative effect on short-term corrosion resistance [24].

There is an evident lack of knowledge about the impact of the LSC on the electrochemical characteristics of magnesium alloys mainly during prolonged exposure periods. Moreover, presented studies used low-powered laser cleaning and reached conclusions opposite to each other. The purpose and novelty of this study are provided by the evaluation of the LSC impact performed using a 100 W power source on corrosion resistance of AZ80 magnesium alloy during the prolonged exposure period in an aggressive chloride environment.

2 Experimental material and methods

The AZ80 magnesium alloy was produced by continuous casting using a heated mould. The chemical composition of AZ80Mg alloy (Table 1) was obtained by EDXRF analysis using ARL QUANT'X EDXRF spectrometer. To observe the microstructure of AZ80, the samples were ground by the SiC papers up to p4000 and polished by polishing cloth using 3 μm and 1 μm polishing emulsions composed of diamond suspension

Table 1 *Chemical composition of AZ31 magnesium alloy obtained by EDXRF analysis*

Component	Al	Zn	Mn	Mg
wt. %	8.99	0.45	0.24	balance

Figure 1 *Pulse laser P-laser, model QFC-100*

and isopropyl alcohol. The samples were then etched for 5 seconds with an etchant consisting of picric acid, acetic acid and ethanol [25]. Microstructural analysis was performed using a Zeiss Axio Imager.A1 optical microscope and corresponding software.

The laser surface cleaning (LSC) treatment was performed using a pulse laser P-laser machine, model QFC-100 (Figure 1). The working distance during the treatment was set at 320 mm. The pulse frequency was 60 Hz and the laser power was 100 W. The pulse duration was 180 ns and the pulse wavelength was λ = 1064 nm. The LSC was applied to the surface for a period of 120 seconds. Each specimen was polished prior to the LSC treatment using the above-mentioned procedure for metallographic analysis to ensure a homogeneous surface before the treatment.

The Alicona InfiniteFocus G5 measuring system was used to evaluate the effect of the LSC treatment and other investigated techniques on morphology and surface roughness. Surface scanning of treated samples was performed within an area of 5 x 5 mm at 10x magnification. The cross-sectional morphology of the treated surfaces was observed using the Zeiss Axio Imager.A1. Moreover, wettability testing was performed using SITA SurfaSpector device.

The electrochemical characteristics of the studied samples were determined by potentiodynamic polarisation (PD) and electrochemical impedance spectroscopy (EIS) using a VSP Biologic VSP 300 laboratory potentiostat, accompanied by EC Lab V11.50 software. Both PD and EIS tests were performed in 0.1 M NaCl solution at the laboratory temperature of 22 ± 2 °C. During the exposures, the samples were stored in corrosion cells as shown in Figure 2. A three-electrode system was used, with the sample acting as the working electrode, the Pt electrode as the auxiliary electrode and the saturated calomel electrode as the reference electrode (+0.2446 V vs. SHE). The PD measurements were started after 10 min of open circuit potential (OCP) stabilisation. In the case of the EIS measurements, the polarisation resistance measurements were made after different OCP stabilization times: 1 h, 2 h, 4 h, 8 h, 12 h, and 24 h in order to observe the electrochemical behaviour during the prolonged exposures.

During the PD tests, samples were polarised in the range -200 mV to +500 mV vs. OCP at a polarisation step rate of 1 $mV.s^{-1}$. The Tafel analysis of the measured PD curves was used to obtain values of corrosion potential (E_{corr}), corrosion current density (i_{corr}), cathodic and anodic coefficients (βc, βa). Corrosion rate values (r_{corr}) were calculated using proper software.

The measured frequencies during the EIS were in the range of 100 kHz to 10 mHz. The amplitude of the applied signal was set at 5 mV with the mean value identical to the OCP value after each exposure period. The measured electrochemical data were plotted as Nyquist plots. These plots were analysed by the equivalent circuit method using two types of equivalent circuit. The first circuit (Figure 3 left) was used to evaluate a simple Nyquist plot with one capacitive loop. The second circuit (Figure 3 right) determined the electrical parameters of the Nyquist diagrams consisting of two capacitive loops. These circuits are used to simulate surface conditions during exposure [16]. The R_{Ω}

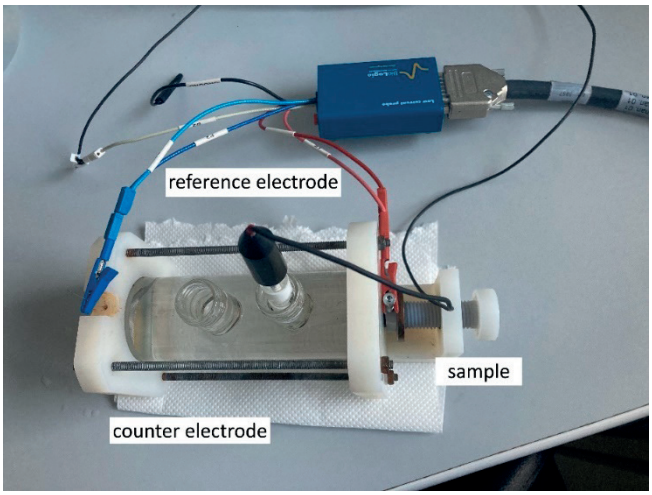

Figure 2 *Corrosion cell*

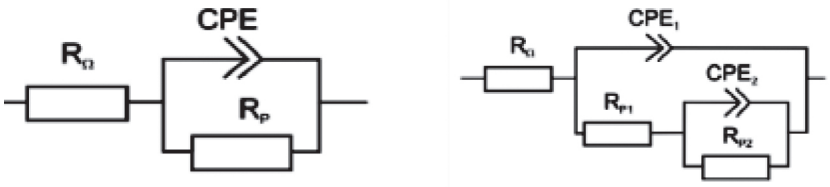

Figure 3 *Equivalent circuits for analysis of Nyquist diagrams with one capacitance loop (left) and two capacitance loops (right)*

component in the circuits is the resistance of the solution and the R_P component determines the polarisation resistance of the surface. Note that the higher the R_P value of the surface, the higher the corrosion resistance. Therefore, this study is mainly oriented to evaluate the corrosion resistance based on the evolution of R_p values during the exposure period. The constant phase element (CPE) represents a heterogeneity of the working electrode (sample) surface. In the case where the Nyquist plot is composed of two capacitance loops, the total polarization resistance is given as the sum of the partial resistances R_{p1} and R_{p2} [26-28].

3 Results and discussion

The microstructure (Figure 4) of the magnesium alloy AZ80 is formed by dendrites of the α-phase. Intermetallic phases were identified based on literature review [26, 29]. The intermetallic phase $Mg_{17}Al_{12}$ is present at the boundaries of dendrites and in interdendritic spaces. The α-phase is a solid solution of aluminium, zinc and manganese in magnesium. An Al_6Mn intermetallic is also present due to the low solubility of manganese in Mg.

The variation of the Sa parameter (arithmetic mean height of the surface) was chosen to determine the roughness after the surface treatments [30]. Table 2 shows that the roughness gradually increased from polished to ground to LSC surface. Note that the roughness values of the polished and ground surfaces were in the same order of magnitude. The roughness value of the surface treated by the LSC method was significantly higher than those of the conventional surface treatments. The LSC surface achieved almost 4 times higher value compared to the polished counterpart.

Figure 5 shows that the polished surface has a typical appearance of a surface treated by mechanical polishing, i.e., it is flat with a low number of heterogeneities such as scratches and pits (Figure $5a_1$). On the ground surface, linear scratches can be seen in the direction of grinding, especially on the top surface view (Figure $5b_1$). The surface roughness was visibly increased compared to polishing, which is well documented in Figure $5b_2$ as well. The appearance of the surfaces treated by LSC is different with respect to those treated by previous methods. When looking at the surface from above (Figure $5c_1$), it is clear that it is directed and regular, corresponding to a pulse laser beam impact applied to the material. Table 2 also shows that as the surface roughness increases, so does the wettability represented by the lower water contact angle values.

The cross sections (Figure 5) show that the surface after the LSC application has not undergone significant melting, as is usually the case with other laser surface treatments such as laser surface melting of magnesium alloys [14]. Therefore, the microstructural appearance of the base material is not visibly affected by this process. On the other hand, the surface is much more heterogeneous compared to the polished and ground counterparts. In addition, the thick porous oxide layer is visible on the surface (Figure $5c_2$) after the LSC application. The oxides formed were heterogeneous and are probably products of the increased reactivity of magnesium with atmospheric oxygen. This is a direct result of the increased temperature of the magnesium base material during the laser treatment.

Potentiodynamic polarisation curves are shown in Figure 6. The electrochemical characteristics were obtained by table analysis of the PD plots (Table 3). Potentiodynamic polarisation curves clearly show that surface roughness and wettability play an important role

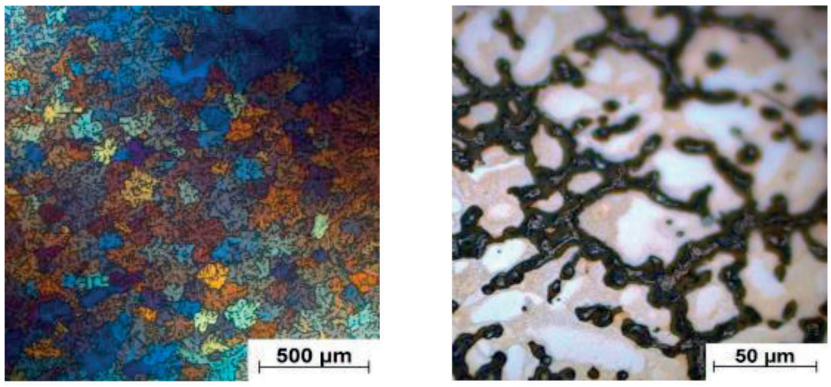

Figure 4 *Microstructure of AZ80 alloy: overview (left) and detail (right)*

Table 2 *Values of the surface roughness and water contact angle of treated samples*

Treatment method	S_a	Contact angle θ, °
Grinding	598.88 nm	52.5 ± 2.6
Polishing	156.49 nm	93.1 ± 1.3
LSC	11.52 µm	42.1 ± 8.8

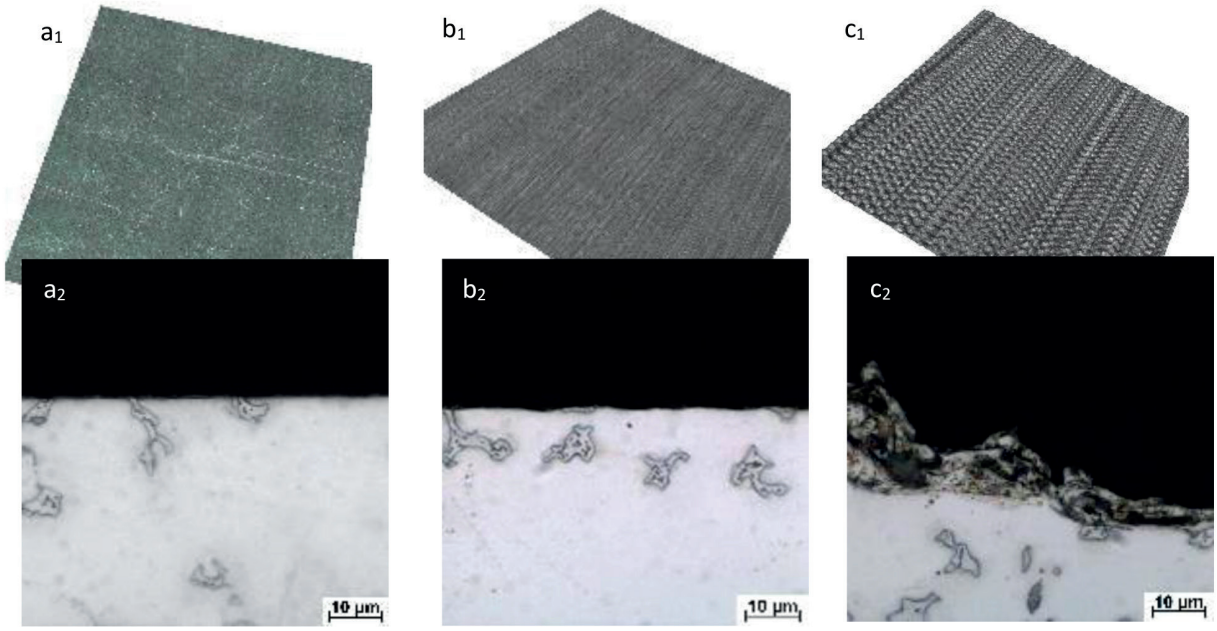

Figure 5 *Surface view (subscript 1) and cross sections (subscript 2)*
a - polishing, b - grinding, c - LSC

Table 3 *Electrochemical characteristics obtained by PD of treated surfaces of AZ80 alloy in 0.1M NaCl*

Treatment method	E_{corr} (mV)	i_{corr} (µA/cm²)	β_a (mV/dec.)	β_c (mV/dec.)	r_{corr} (mm/year)
Grinding	-1525 ± 13	8 ± 1	57 ± 13	157 ± 6	0.19 ± 0.02
Polishing	-1509 ± 19	7 ± 1	128 ± 19	153 ± 1	0.16 ± 0.01
LSC	-1568 ± 3	13 ± 1	82 ± 6	139 ± 4	0.29 ± 0.03

in the corrosion behaviour [7, 30]. The surface treated by the LSC method showed the lowest values of corrosion potential (E_{corr}), indicating the lowest thermodynamic stability of the surface. The most thermodynamically stable surface was the one treated by polishing. In terms of corrosion current density (i_{corr}) and corrosion rate (r_{corr}), the LSC treated samples reached the highest values of these electrochemical characteristics. Note that these characteristics represent corrosion kinetics in such a way that the higher these values are, the more intense the corrosion degradation is [31]. On the other hand, the i_{corr} and r_{corr} for polished and ground surfaces were not significantly different. The main reason for the reduced corrosion resistance of the LSC samples is the presence of the increased electrochemically active area in contact with aggressive environment confirmed by roughness measurement (Table 2). In addition, the porous and non-compact oxide layer formed on the surface (Figure $5c_2$) does not provide a sufficient barrier effect. The effect of surface roughness on the corrosion resistance has been investigated by several authors [7, 30]. In the first case, Reddy et al., 2021 investigated the effect of milling feed rate on roughness and corrosion behaviour of magnesium alloy. The authors found that an increase in surface roughness promoted corrosion degradation [7]. In a second study, the authors demonstrated that decreasing the surface roughness led to the more noble values of corrosion potential [30]. The Figure 6 shows that the potentiodynamic curves for polished and lasered surfaces are of similar shape, which means that the surface reacts similarly to polarisation. However, the values of E_{corr} are different. In accordance with the above-mentioned study of Walter et al., 2011 [30], the rougher surface after LSC resulted in more negative values of E_{corr}, meaning worse thermodynamic stability. It can be assumed that the surface film containing oxides (MgO), hydroxides ($Mg(OH)_2$ and $MgCl_2$ was formed on all tested surfaces during exposure to 0.1M NaCl solution [1, 13]. The factor that made the difference between the samples is the initial roughness of the surface on which this film is formed. The rougher the surface, the more difficult it is to form a compact homogeneous surface film. This phenomenon contributed to the higher corrosion resistance of the polished surface [7, 30, 32].

Another factor to consider when talking about corrosion resistance is the surface wettability. Table 2 shows that high roughness values are associated with increased surface wettability. It can be seen that as the roughness increases the water contact angle decreases. It can be seen that this fact results in an enhanced retention of a water/electrolyte drop on the surface and such surface conditions are favourable for corrosion initiation [1-2, 7, 33].

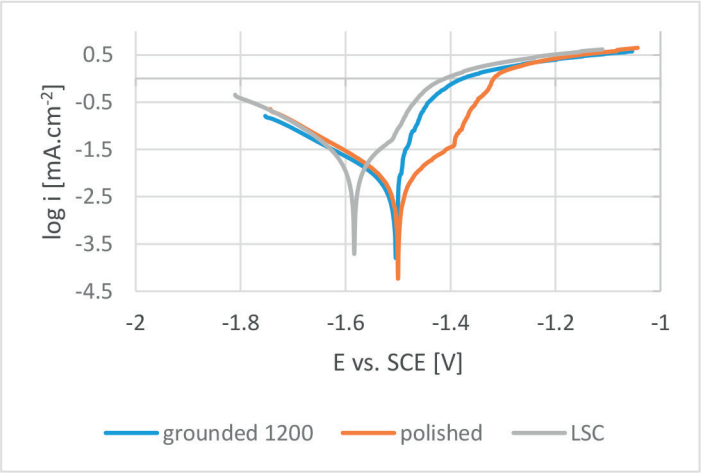

Figure 6 *Representative potentiodynamic polarization curves of treated surfaces of AZ80 alloy tested in 0.1M NaCl solution*

Table 4 *Polarization resistance of treated surfaces of AZ80 alloy in 0.1M NaCl*

Treated method	R_p (Ω.cm²)					
	1 h	2 h	4 h	8 h	12 h	24 h
Grounded	3817	3410	2577	2268	2210	1769
Polished	13770	9376	9070	7544	7191	6961
LSC	655	671	650	740	682	549

For the EIS test, a prolonged exposure of up to 24 hours was set to observe the corrosion behaviour of the treated surfaces in an aggressive corrosive environment represented by 0.1M NaCl. The R_p values (Table 4), obtained by equivalent circuit analysis of the Nyquist plots (Figure 7), describe the electrochemical stability of the surface, as these values are directly proportional to the corrosion resistance of the corresponding surface. The Nyquist plots show that only the polished surface is represented by the two capacitance loops, corresponding to the formation of a more compact oxide/hydroxide surface layer compared to ground and LSC samples. These oxides formed a film that suppressed the corrosion process in the first hour of exposure (Table 4). However, such surface film did not play a significant role in the overall corrosion resistance. This oxide/hydroxide film is not able to slow down the corrosion process as these substances are only stable in alkaline environments [1, 12, 30].

It is clear that after the first hour of exposure, the most resistant surface was the polished surface and the lowest corrosion resistance was measured in the case of the LSC treated surface. This result is in good agreement with the presented results of the PD tests (Figure 6, Table 2). On the other hand, the LSC treated surface was the only one to show an increase of the R_P during the prolonged exposure. This improvement in corrosion resistance over time can be explained by the local sealing of the porous oxidic film formed during the laser treatment (Figure $5c_2$) by the products of the corrosion reactions. The maximum R_P was obtained after 8 hours of exposure, followed by a continuous decrease in corrosion resistance due to the instability of the porous layer of corrosion products mentioned above. In contrast, the polished and ground samples showed a decrease in corrosion resistance throughout the exposure period, indicating continuous corrosion degradation. Note that the two conventional treatments reached higher corrosion resistance compared to LSC, with the polished surface showing the highest electrochemical stability throughout the exposure.

Based on the principle of the LSC method, it can be assumed that the lasered surface layer exhibited increased internal energy leading to a promoted surface reactivity. Consequently, the creation of oxides/hydroxides by reaction with the surrounding atmosphere leading to the formation of surface film and corrosion products during exposure, was catalysed. Sealing of the oxide/hydroxide surface film happened more easily on heterogeneous surface due to the presence of capillaries and irregularities within the original surface film on the LSC surface (Figure $5c_2$) [1, 13, 34]. Similarly, to the previous case, the created film and products of corrosion reactions are not protective in neutral pH environment for longer period and will naturally deteriorate, which is demonstrated by decreasing trend of the R_p values after 12 h of exposure [1]. The obtained LSC results can be compared to another unconventional method of surface treatment such as shot peening. Although this method works on different principles, the resulting surface is similar when speaking about heterogeneity of surface and corrosion behaviour. Comparably to the LSC, the oxide film is formed on the surface during the shot peening treatment. Internal energy of the surface is

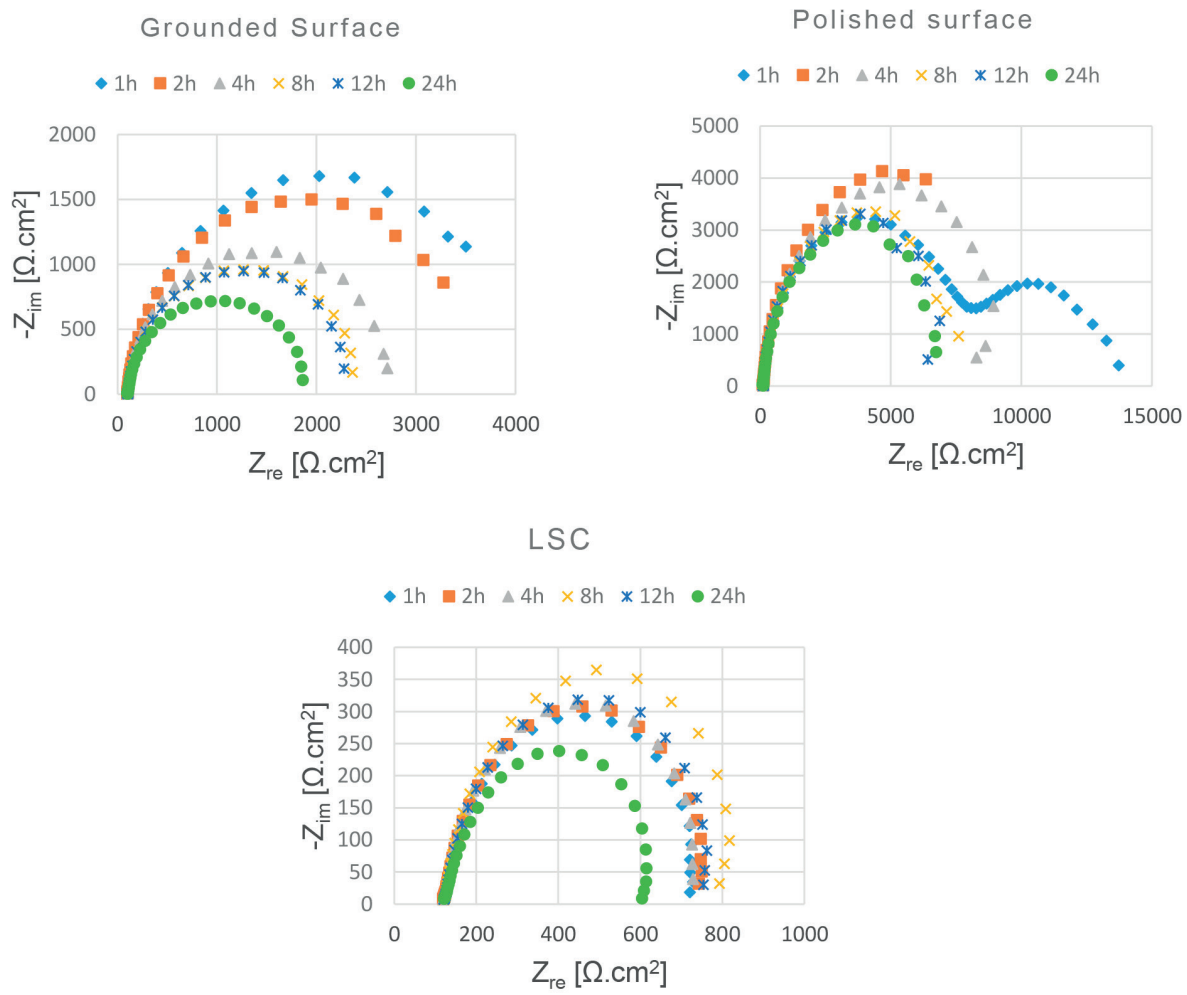

Figure 7 *Nyquist diagrams of treated surfaces of AZ80 alloy tested in 0.1M NaCl*

amplified by the intensive plastic deformation resulting in promoted oxidation of substrate and decreased corrosion resistance [30-31, 35].

Although the LSC method at selected parameters did not improve the corrosion resistance of the AZ80 magnesium alloy in the desired way, there is considerable scope for developing this method in terms of its optimization. The modification of the ablation process is possible on multiple levels - adjusting the device's power, defocusing the laser beam to achieve lower beam intensity to achieve more uniform 100% coverage with lower roughness. On the other hand, obtained results can be exploited for further research connected with coatings as the rough and reactive surface provides suitable thermodynamic conditions for the formation of oxide protective layers such as plasma electrolytic oxidation or anodization [13].

4 Conclusions

The performed experiments were designed to compare conventional and unconventional surface treatment methods. The following conclusions were drawn from the obtained results:

The highest roughness and promoted wettability were obtained by the LCS treated surface. Microscopic observations revealed that the LSC surface showed an oxidised heterogeneous layer after the treatment.

Potentiodynamic polarization experiments confirmed the relationship between the surface roughness, wettability and corrosion resistance. The lowest corrosion resistance was measured on the LSC treated surface; the highest corrosion resistance was recorded on the polished surface.

Electrochemical impedance spectroscopy experiments confirmed the results of the PD tests. After the first hour of exposure, the difference between the LSC surface and the polished surface was significant. The EIS tests also showed that the LSC surface exposed to an NaCl solution underwent passivation leading to an increase of the R_p up to 8 hours of exposure. However, the highest R_p values during the exposure period were obtained from the polished surface. The LSC surface showed the lowest corrosion resistance after 24 hours of exposure.

Acknowledgement

The research was funded by the EU NextGenerationEU through the Recovery and Resilience Plan for Slovakia under the project No. 09I03-03-V03-00036.

Conflicts of interest

The authors declare that they have no known competing financial interests or personal relationships that could have appeared to influence the work reported in this paper.

References

[1] SONG, G. L. *Corrosion of magnesium alloys*. 1. ed. Philadelphia: Woodhead Publishing, 2011. ISBN 978-1-84569-708-2.

[2] JIANG, J., GENG, X., ZHANG, X. Stress corrosion cracking of magnesium alloys: a review. *Journal of Magnesium and Alloys* [online]. 2023, **11**(6), p. 1906-1930. eISSN 2213-9567. Available from: https://doi.org/10.1016/j.jma.2023.05.011

[3] SANDLOBES, S., FRIAK, M., KORTE-KERZEL, S., PEI, Z., NEUGEBAUER, J., RAABE, D. A rare-earth free magnesium alloy with improved intrinsic ductility. *Scientific Reports* [online]. 2017, **7**, 10458. eISSN 2045-2322. Available from: https://doi.org/10.1038/s41598-017-10384-0

[4] LIU, B., YANG, J., ZHANG, X., YANG, Q., ZHANG, J., LI, X. Development and application of magnesium alloy parts for automotive OEMs: a review. *Journal of Magnesium and Alloys* [online]. 2022, **11**(1), p. 15-47. eISSN 2213-9567. Available from: https://doi.org/10.1016/j.jma.2022.12.015

[5] WHITE, L., KOO, Y., YUN, Y., SANKAR, J. TiO2 deposition on az31 magnesium alloy using plasma electrolytic oxidation. *Journal of Nanomaterials* [online]. 2013, **2013**, 19437. ISSN 1687-4110, eISSN 1687-4129. Available from: https://doi.org/10.1155/2013/319437

[6] DING, Y., WEN, C., HODGSON, P., LI, Y. Effects of alloying on corrosion behavior and biocompatibility of biodegradable magnesium alloys: a review. *Journal of Materials and Chemistry B* [online]. 2014, **2**, p. 1912-1933. ISSN 2050-750X, eISSN 2050-7518. Available from: https://doi.org/10.1039/C3TB21746A

[7] REDDY, U., DUBEY, D., PANDA, S. S., IREDDY, N., JAIN, J., MONDAL, K., SINGH, S. S. Effect of surface roughness induced by milling operation on the corrosion behavior of magnesium alloys. *Journal of Materials Engineering and Performance* [online]. 2021, **30**, p. 7354-7364. ISSN 1059-9495, eISSN 1544-1024. Available from: https://doi.org/10.1007/s11665-021-05933-8

[8] ATRENS, A., SONG, G.-L., LIU, M., SHI, Z., CAO, F., DARGUSH, M. S. Review of recent developments in the field of magnesium corrosion. *Advanced Engineering Materials* [online]. 2015, **17**(4), p. 400-453. ISSN 1438-1656, eISSN 1527-2648. Available from: https://doi.org/10.1002/adem.201400434

[9] FINTOVA, S., DRABIKOVA, J., PASTOREK, F., TKACZ, J., KUBENA, I., TRSKO, L., HADZIMA, B., MINDA, J., DOLEZAL, P., WASSERBAUER, J., PTACEK, P. Improvement of electrochemical corrosion characteristics of AZ61 magnesium alloy with unconventional fluoride conversion coatings. *Surface and Coatings Technology* [online]. 2019, **357**, p. 638-650. ISSN 0257-8972, eISSN 1879-3347. Available from: https://doi.org/10.1016/j.surfcoat.2018.10.038

[10] YOUSSEF, H., EL-HOFY, H. *Traditional machining technology* [online]. Boca Raton: CRC Press, 2020. ISBN 9781003055303. Available from: https://doi.org/10.1201/9781003055303

[11] CZAN, A., JOCH, R., SAJGALIK, M., HOLUBJAK, J., HORAK, A., TIMKO, P., VALICEK, J., KUSNEROVA, M., HARNICAROVA, M. Experimental study and verification of new monolithic rotary cutting tool for an active driven rotation machining. *Materials* [online]. 2022, **15**, 1630. eISSN 1996-1944. Available from: https://doi.org/10.3390/ma15051630

[12] VICEN, M., BOKUVKA, O., SKOVAJSA, M., NOVY, F., FLORKOVA, Z. Energy-efficient application of CrN coating on low-alloy tool steel: comparative analysis of technological processes. *Production Engineering Archives* [online]. 2024, **30**(3), p. 406-412. ISSN 2353-5156, eISSN 2353-7779. Available from: https://doi.org/10.30657/pea.2024.30.39

[13] KAJANEK, D., PASTOREK, F., HADZIMA, B., BAGHERIFARD, S., JAMBOR, M., BELANY, P., MINARIK, P. Impact of shot peening on corrosion performance of AZ31 magnesium alloy coated by PEO: comparison with conventional surface pre-treatments. *Surface and Coatings Technology* [online]. 2022, **446**, 128773. ISSN 0257-8972, eISSN 1879-3347. Available from: https://doi.org/10.1016/j.surfcoat.2022.128773

[14] HU, R., ZHANG, S., BU, J.-F., LIN, CH.-J., SONG, G.-L. Recent progress in corrosion protection of magnesium alloys by organic coatings. *Progress in Organic Coatings* [online]. 2012, **73**(2-3), p. 123-141. ISSN 0300-9440, eISSN 1873-331X. Available from: https://doi.org/10.1016/j.porgcoat.2011.10.011

[15] ZHANG, F. D., LIU, H., SUBKA, C., LIU, Y. X., LIU, Y., GUO, W., CHENG, Y. M., ZHANG, S. L., LI, L. Corrosion behaviour of laser-cleaned AA7024 aluminium alloy. *Applied Surface Science* [online]. 2018, **435**, p. 452-461. ISSN 0169-4332. ISSN 0169-4332, eISSN 1873-5584. Available from: https://doi.org/10.1016/j.apsusc.2017.11.141

[16] DOBREV, T., PHAM, D. T., DIMOV, S. S. Laser polishing. In: Second International Conference on Multi-Material Micro Manufacture: proceedings[online]. Elsevier Science. 2019. ISBN 978-0-08-045263-0. Available from: https://doi.org/10.1016/B978-0-08-045263-0.X5000-4

[17] GUAN, Y. C., ZHOU, W., ZHENG, H. Y. Effect of laser surface melting on corrosion behaviour of AZ91D Mg alloy in simulated-modified body fluid. *Journal of Applied Electrochemistry* [online]. 2009, **39**, p. 1457-1464. ISSN 0021-891X, eISSN 1572-8838. Available from: https://doi.org/10.1007/s10800-009-9825-2

[18] TAN, Y. C., WEN, C., ANG, H. O. Influence of laser parameters on the microstructures and surface properties in laser surface modification of biomedical magnesium alloys. *Journal of Magnesium and Alloys* [online]. 2024, **22**(1), p. 72-97. eISSN 2213-9567. Available from: https://doi.org/10.1016/j.jma.2023.12.008

[19] HEIDELMANN. G. Surface cleaning with laser technology. *Plating and Surface Finishing*. 2009, p. 38-41. ISSN 03603164.

[20] HYOUNGWON, P., YOO, H. J., PARK, CH. Wear and corrosion behaviors of high-power laser surface-cleaned 304L stainless steel. *Optics and Laser Technology* [online]. 2024, **168**, 109640. ISSN 0030-3992, eISSN 1879-2545. Available from: https://doi.org/10.1016/j.optlastec.2023.109640

[21] WANG, W., LI, X., LIU, W., XING, F., WANG, J., ZHANG, K. Experimental study on hydrophobic properties and corrosivity of laser cleaned 7075 aluminum alloy anodized film surface. *Optics and Laser Technology* [online]. 2023, **166**, 109615. ISSN 0030-3992, eISSN 1879-2545. Available from: https://doi.org/10.1016/j.optlastec.2023.109615

[22] PROKURATOV, D., SAMOKHVALOV, A., PANKIN, D., VERESHCHAGIN, O., KURGANOV, N., POVOLOTCKAIA, A., SHIMKO, A., MIKHAILOVA, A., BALMASHNOV, R., SMOLYANSKAYA, O., REDKA, D., SALGALS, T., BOBROVS, V. Laser irradiation effects on metallic zinc and its corrosion products. *Journal of Cultural Heritage* [online]. 2023, **61**, p. 13-22. ISSN 1296-2074, eISSN 1778-3674. Available from: https://doi.org/10.1016/j.culher.2023.02.003

[23] ZHU, H., WU, CH., XUE, L., YANG, L., LIU, Y., WANG, D., LIANG, Y., PENG, Z. Effect of laser cleaning on the growth and properties of micro-arc oxidation layers of AZ31 magnesium alloy. *Surface and Coatings Technology* [online]. 2024, **488**, 131051. ISSN 0257-8972, eISSN 1879-3347. Available from: https://doi.org/10.1016/j.surfcoat.2024.131051

[24] XIONG, W., FU, J., LIU, CH., LI, L., WANG, H., ZHANG, M., GE, Z., ZHANG, T., WANG, Q. Laser-chemical surface treatment for enhanced anti-corrosion and antibacterial properties of magnesium alloy. *Coatings* [online]. 2024, **14**(3), 287. eISSN 2079-6412. Available from: https://doi.org/10.3390/coatings14030287

[25] MOFID, M. A., LORYAEI, E. Investigating microstructural evolution at the interface of friction stir weld and diffusion bond of Al and Mg alloys. *Journal of Materials and Research and Technology* [online]. 2019, **8**(5), p. 3872-3877. ISSN 2238-7854, eISSN 2214-0697. Available from: https://doi.org/10.1016/j.jmrt.2019.06.049

[26] KAJANEK, D., HADZIMA, B., PASTOREK, F. Electrochemical characterization of AZ31 magnesium alloy treated by ultrasonic impact peening (UIP). *Communications - Scientific Letters of the University of Zilina* [online]. 2018, **20**(3), p. 24-29. ISSN 1335-4205, eISSN 2585-7878. Available from: https://doi.org/10.26552/com.C.2018.3.24-29

[27] PASTOREK, F., STRBAK, M., KAJANEK, D., JACKOVA, M., PASTORKOVA, J., FLORKOVA, Z. Corrosion behaviour of preserved PEO coating on AZ31 magnesium alloy. *Communications - Scientific Letters of the University of Zilina* [online]. 2021, **23**(2), p. B76-B88. ISSN 1335-4205, eISSN 2585-7878. Available from: https://doi.org/10.26552/com.C.2021.2.B76-B88

[28] KAJANEK, D., HADZIMA, B., BREZINA, M., JACKOVA, M. Effect of applied current density of plasma electrolytic oxidation process on corrosion resistance of AZ31 magnesium alloy. *Communications - Scientific Letters of the University of Zilina* [online]. 2019, **21**(2), p. 32-36. ISSN 1335-4205, eISSN 2585-7878. Available from: https://doi.org/10.26552/com.C.2019.2.32-36

[29] ESMAILY, M., SVENSSON, J. E. FAJARDO, S., BIRBILIS, N., FRANKEL, G. S., VIRTANEN, S., ARRABAL, R., THOMAS, S., JOHANSSON, L. G. Fundamentals and advances in magnesium alloy corrosion. *Progress in Materials Science* [online]. 2019, **89**, p. 92-193. ISSN 0079-6425, eISSN 1873-2208. Available from: https://doi.org/10.1016/j.pmatsci.2017.04.011

[30] WALTER, R., KANNAN, M. B. Influence of surface roughness on the corrosion behaviour of magnesium alloy. *Materials and Design* [online]. 2011, **32**(4), p. 2350-2354. ISSN 0261-3069. Available from: https://doi.org/10.1016/j.matdes.2010.12.016

[31] KHOSHNAW, F., GUBNER, R. Corrosion atlas case studies part i: general aspects of corrosion, corrosion control, and corrosion prevention. In: *Corrosion atlas series* [online]. Elsevier, 2020. ISBN 9780128187609. Available from: https://doi.org/10.1016/B978-0-12-818760-9.02002-X

[32] PASTOREK, F., HADZIMA, B., KAJANEK, D. *Preparation and corrosion properties of structural materials with refined grain structure*. Harlow: Person, 2019. ISBN 978-8396-1054-7.

[33] BERTOLINI, R., BRUSCHI, S., GHIOTTI, A., PEZZATO, L., DABALA, M. The effect of cooling strategies and machining feed rate on the corrosion behavior and wettability of AZ31 alloy for biomedical applications. *Procedia CIRP* [online]. 2017, **65**, p. 7-12. eISSN 2212-8271. Available from: https://doi.org/10.1016/j.procir.2017.03.168

[34] LI, W., LI, D. Y. Influence of surface morphology on corrosion and electronic behavior. *Acta Materialia* [online]. 2006, **54**(2), p. 445-452. ISSN 1359-6454, eISSN 1873-2453. Available from: https://doi.org/10.1016/j.actamat.2005.09.017

[35] BAGHERIFARD, S., HICKEY, D. J., FINTOVA, S., PASTOREK, F., FERNANDEZ-PARIENTE, I., BANDINI, M., WEBSTER, T. J., GUAGLIANO, M. Effects of nanofeatures induced by severe shot peening (SSP) on mechanical, corrosion and cytocompatibility properties of magnesium alloy AZ31. *Acta Biomaterialia* [online]. 2018, **66**, p. 93-108. ISSN 1742-7061. ISSN 1742-7061, eISSN 1878-7568. Available from: https://doi.org/10.1016/j.actbio.2017.11.032